# AIREON SPACE BASED ADS-B PERFORMANCE MODEL

*Dr. Michael A. Garcia, Aireon, McLean, VA*
*James Stafford and Dr. Jay Minnix, Exelis, Herndon, VA*
*John Dolan, Regulus, Washington, DC*

## Abstract

Global, continuous, low-latency, and high performance surveillance of aircraft via Space-Based ADS-B (Automatic Dependent Surveillance Broadcast) is an emerging technology for the aviation industry. The Iridium-NEXT Low Earth Orbit (LEO) satellites, which will host the Aireon ADS-B receiver payloads, will begin launching in 2015 with all 66 operational satellites in their mission orbit by 2017, gradually replacing the current Iridium satellite constellation and enabling the global ADS-B surveillance services of Aireon [1- 3].

Prior to launch, a series of system and receiver models, simulations, and studies were produced in order to estimate metrics of this unique surveillance system such as the expected ADS-B aircraft position update interval. To assess whether the required update intervals for providing aircraft separation services will be achievable, the density of aircraft and other 1090 MHz in-band transmitters must be taken into account with respect to the large satellite beam footprints as a function of time and space (particularly near coastal areas where air traffic is most dense). This work describes a model for calculating the expected impact of aircraft density, mixed avionics equipage, and satellite motion on the ADS-B update interval performance for wide area space-based receiver systems. Additionally, several examples of expected performance based on the model are characterized in various Flight Information Regions (FIRs).

## I. Introduction

Once the Aireon system is certified for Air Traffic Control (ATC) operations in 2018, it is estimated by fast time simulation modeling that annual savings of several hundreds of millions of dollars in fuel are possible through optimal climbs and more efficient routes enabled by Space-Based ADS-B surveillance. Aireon will provide a safety-case driven, enterprise-class ADS-B surveillance service to many areas that have no surveillance today. Other offerings include gap-filler, contingency and remote asset reduction solutions for customers that already have some surveillance in their area.

The current air traffic management (ATM) environment is based on the aircraft capability to navigate to a destination, communicate to an air traffic controller, and to participate in cooperative surveillance to air traffic control for separation and situational awareness services. Cooperative aircraft surveillance uses a variety of technologies both legacy and modern, which leads to a mixture of in-band spectrum occupancy from avionics. ADS-B is the most modern of the established aircraft surveillance technologies and will soon be installed and operational on the majority of controlled aircraft by 2020 in order to comply with mandates set by the US, Europe, Australia, and many other regions.

Although there are several links associated with ADS-B, 1090 Extended Squitter (1090ES) will be the most common equipage, particularly amongst airline operators and others that fly above 18,000 ft. 1090ES ADS-B is the internationally harmonized datalink approved by ICAO and documented in the Standards and Recommended Practices (SARPS) to be compatible for worldwide use. 1090ES ADS-B avionics broadcast messages on 1090 MHz and successful reception of these messages depends on the signal to noise ratio and the channel occupancy which is affected by ADS-B and other 1090 MHz signals above the receiver's sensitivity. This paper focuses on the latter of these two factors since it is more challenging to predict its impact on Space Based ADS-B performance.

## II. ADS-B Co-Channel Interference

FRUIT (False Replies Uncorrelated In Time) is a "catch-all" term commonly used in the ATC industry to refer to 1090 MHz co-channel interference from a mix of 1090 MHz avionics and devices [4]. The following aircraft avionics are considered significant contributors to a FRUIT (i.e. co-channel interference) environment:

978-1-4799-8952-2/15/$31.00 ©2015 IEEE

1. ATCRBS and IFF
2. Mode S
3. 1090ES ADS-B

Each of these avionics link technologies has different characteristics individually, yet typically combines together with the others as an aggregate to degrade the reception of desired 1090ES ADS-B aircraft messages [5]. Although there are other link technologies near 1090 MHz, these three groups are considered to have the most impact to ADS-B reception [6].

### *ATCRBS and IFF*

Air Traffic Control Radar Beacon System (ATCRBS) is one of the oldest aircraft surveillance link communication schemes [7]. The encoding and behavior of ATCRBS is based on the Identification Friend or Foe (IFF) system used during World War II [8]. ATC radars will interrogate using ATCRBS calling signals at 1030 MHz and the ATCRBS avionics will reply on 1090 MHz with a pulse amplitude modulated (PAM) signal that has a duration of about 20 μs. Each ATCRBS message only tells the recipient either the four digit octal identifier (Mode 3/A reply) or the altitude (Mode C reply) of the aircraft.

Military ATCRBS protocols Mode 1 and Mode 2 replies have the same duration as the Mode 3/A and Mode C replies (20 μs) and the Mode 4 message duration is only 3.6 μs and can therefore be modelled similarly to that of the civilian ATCRBS messages. Mode 5 has Level 1 replies, which are 15 μs in duration, and Level 2, which are 35 μs and can therefore also be considered analogous to ATCRBS in terms of its impact to ADS-B reception [9]. The Joint Tactical Information Distribution System (JTIDS) Link 16 is another military IFF communication scheme that falls in the same UHF L band as 1090 MHz, however the JTIDS Link 16 RF transmissions are assumed to be part of the Gaussian noise background since they are at least 22 MHz away from 1090 MHz [10, 11]. In general, according to ICAO Annex 10 Vol IV section 3.1.2.3.2.4, military applications are provisioned to ensure that they do not exceed the RF power and reply/squitter rate requirements levied on the civil IFF systems [12].

Many ATCRBS surveillance systems end up requesting multiple replies from aircraft using doublet and triplet schemes in order to improve the reliability of the receptions and correlations of aircraft replies at the radars. In a densely populated area with multiple radars operating within a few 100 nautical miles of each other: several radars, multi-lateration systems, and other aircraft-based surveillance systems such as the Traffic Collision Avoidance System (TCAS) will make their own independent requests for ATCRBS replies, resulting in escalating 1090 MHz transmission rates.

### *Mode S*

Mode S was introduced in the 1960s as an update to ATCRBS avionics [13]. The link scheme was greatly improved from ATCRBS including Cyclic Redundancy Checks (CRC), increased number of bits per message (56 instead of 12), and the use of pulse position modulation (PPM) instead of PAM. Additionally, every Mode S message contains a globally unique ID of the aircraft known as the ICAO or 24-bit Target Address, vastly improving message-to-message correlation. This permitted radar and aircraft surveillance systems to lower their overall rates of interrogations and thus elicits of replies. However, all of these radar and aircraft systems were still independent of each other and thus still resulted in a large amount of redundant messaging per aircraft.

### *1090ES ADS-B*

1090ES ADS-B was introduced and developed in the 1990s largely based on the Mode S messaging scheme [14]. The key difference being that neither ground nor airborne systems could request transmissions from these avionics, but rather the avionics would *automatically broadcast* their replies based with pseudorandom time intervals between each message. These long messages (112 bits) also contain aircraft state vector information that conveys the aircraft's navigation information from its on-board Global Navigation Satellite System (GNSS) directly to any 1090ES ADS-B receivers. The communication of state vector information practically eliminates the need for any interrogation since the plane has determined its own position via GNSS and is conveying that to the ADS-B 1090ES receivers. The aircraft's encoded position can be verified through methods such as time difference of arrival

(TDOA) from multiple ground stations and/or low frequency interrogation surveillance. Therefore, the 1090ES ADS-B protocol has a relatively static, per-aircraft channel occupancy rate and increased adoption of ADS-B will eventually reduce the Mode S and ATCRBS reply rates exhibited today [15].

## III. Approach

In order to produce a FRUIT/interference environment model that isn't overly-conservative nor overly-optimistic it was decided to use a bottom's up approach to build an "organic" FRUIT environment derived from historical global flight plan data [16]. The central question being asked of the FRUIT model is:

> "If a Space-Based ADS-B (SBA) receiver has a phased array high gain beam pointed at a particular place on the globe at a particular time and the spatial gain contours of the beam are known, how will FRUIT impact the expected probability of successful reception and decoding of an ADS-B message, $P_d$, at a given location?"

The most commonly used approach when modeling FRUIT is to assume that its effect corresponds to a Poisson Arrival Rate behavior [17]. The assumption of a Poisson Arrival Rate system is that the messaging scheme corresponds to that of a random access channel. A random access channel is a relatively cheap and efficient means of communication since time-synchronization is not required of the transmitter or the receiver. For the conservative case of a channel with perfect reception of non-interfered messages and zero reception of overlapped messages: as the offered load, *G*, increases, the detection probability of a message decreases exponentially, i.e. $P_{msg} = e^{-K*G}$ (See Figure 1). Mode S (K = 1.5), ATCRBS (K = 1.17), and Mode 4 (K = 1.03) all have shorter message durations than ADS-B (K = 2), hence the improved ADS-B $P_d$ in those environments as it relates to the co-channel load factor.

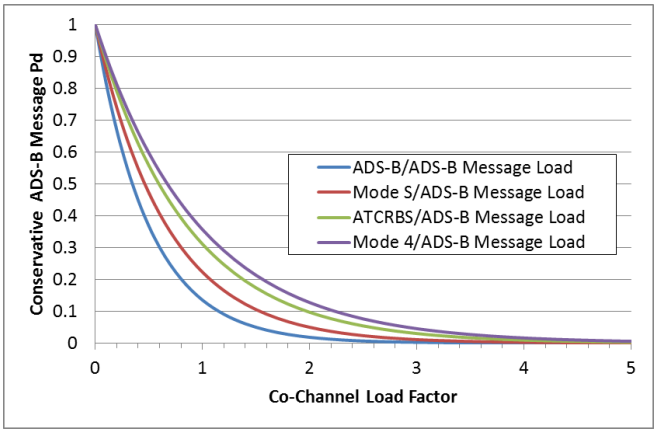


**Figure 1. General Poisson Arrival Rate Curves**

In order to account for the complexity specific to ADS-B message reception as it relates to ATCRBS, Mode S, and other 1090ES ADS-B transmissions, we start with $P_R$, the probability of successful reception of an ADS-B message in a "Clear Sky" environment (i.e. without FRUIT).

Then we make assumptions about the probability of successful reception in the presence of given number $n$ of interfering messages of the various types. For Mode S and ES messages, it is assumed that only zero overlap is tolerable for the ADS-B message and that "room" in time must be created for it. This is a fairly conservative assumption given the known ADS-B message bit error correction techniques described in Appendix I of DO-260B [14], but allows for additional unknown short-burst error quantities to be left out of the calculation (e.g. in-band DME/TACAN transmissions). The probability of reception given $n$ interfering arrivals is therefore assumed to be

$$P_{Mode\ S,ES}(R|n) = \begin{Bmatrix} P_R & n = 0 \\ 0 & n > 0 \end{Bmatrix}$$

and for ATCRBS we assume the minimal probability of reception for A1 class receivers with zero to three overlapping ATCRBS messages as specified by the standards (Table 2-168, page 591 of section 2.4.4.4.2.4 [14, 18]), specifically

$$P_{ATCRBS}(R|n) = \begin{Bmatrix} P_R & n = 0 \\ 0.89P_R & n = 1 \\ 0.64P_R & n = 2 \\ 0.52P_R & n = 3 \\ 0 & n > 3 \end{Bmatrix}$$

As mentioned above, we assume that the arrivals of each interfering message follow a Poisson arrival process. For such a process with parameter $\lambda$, the number of arrivals is

$$P_\lambda(n) = \frac{\lambda^n}{n!} e^{-\lambda}$$

Finally, we assume that the three classes of interfering signal arrive independently of each other, such that $P_d = P_R \cdot P_{ATCRBS} \cdot P_{ES} \cdot P_{ModeS}$ [16]. The effects of these message loads on ADS-B Pd in one beam can be viewed in isolation in Figure 2.

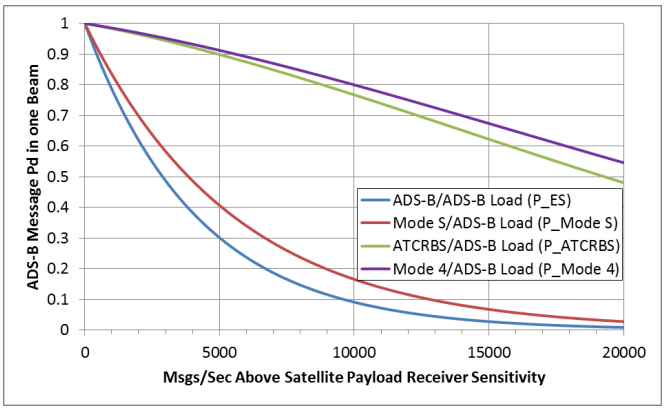


**Figure 2. ADS-B Msg $P_d$ vs. Msg Arrival Rate**

Putting all these assumptions together leads to equation (1) which is the basis of our model:

$$P_d = P_R \cdot \left(1 + 0.89\lambda_{ATCRBS} + \frac{0.64}{2}\lambda_{ATCRBS}^2 + \frac{0.52}{6}\lambda_{ATCRBS}^3\right) \cdot e^{-(\lambda_{ATCRBS}+\lambda_{ES}+\lambda_{ModeS})} \quad (1)$$

Eq. 1 can be summarized as $P_d = P_R \cdot P_{env}$

- The $\lambda$ terms are the offered load values for each respective link technology.
- For example, $\lambda_{ModeS}$ is the expected offered load of the Mode S messages (normalized to account for signal fading) as the ADS-B message of interest where $\lambda_{ModeS} = \varphi_{ModeS} \cdot \tau_{ModeS}$, and $\varphi_{ModeS}$ is the Mode S arrival rate (messages/sec) within the signal reception range of the SBA receiver and $\tau_{ModeS}$ is the duration of each Mode S message plus the duration of a 1090ES message (64 + 120µs)

The duration values are assumed to be as follows: $\tau_{ATCRBS}$ = 141 µs, $\tau_{ModeS}$ = 184 µs, and $\tau_{ES}$ = 240 µs.

An attenuation penalty is also applied as a function of elevation, $\alpha$, in order to determine the relative gain from a bottom antenna squitter versus a top antenna (for a TLAT style antenna [19], $\beta_{bottom} = \beta_{top} - 0.373\alpha$ in dB, where $\alpha$ is in degrees). In particular, this bottom antenna squitter attenuation penalty seems to have been overlooked by several other analysis papers on SBA compatibility with legacy surveillance systems, which can lead to overly pessimistic conclusions regarding performance [20].

The only unknowns in this equation are the $\varphi$ values. It is assumed that FRUIT has an independent "field effect" on each SBA receiver beam. This means that each beam can be handled such that the combined effect of the FRUIT impacts any and all other received ADS-B messages with the same "penalty" ($P_{env}$). This assumption is rooted in the idea that $\varphi$ can be calculated using a tile/grid based approach over the earth's surface with the beam gain contours applying a respective weight to each grid point. In this way, an *effective* arrival rate can be calculated as such:

$$\varphi_{ModeS}(h) = \sum_{i=1}^{n} \varphi_{ModeS}(h, t_i) \cdot \gamma_{t_i}$$

where h is the hour in the simulation (this model assesses peak aircraft density on an hourly basis), and $t_i$ is the i$^{th}$ tile of the observable n tiles during simulation hour h. The gain or weighting factor $\gamma_{t_i}$ is based on the SBA receiver's Message Error Rate (MER) relationship to the energy per bit relative to the noise floor ($E_b/N_0$) calculated at the i$^{th}$ tile for a particular beam during hour *h*. In Aireon's case, the beam gain patterns and MER curves are based on Harris's model of their advanced SBA receiver.

Typically, the $E_b/N_0$ link budget will be calculated to a tile from the satellite as a function of range, azimuth and elevation to a 125W aircraft transmitter. An increase in transmitter power improves the $E_b/N_0$ by 3 dB (250W) or 6 dB (500W).

## IV. Description of Assumptions

### *Spatial/Temporal Aircraft Counts*

In alignment with the ATM industry, this FRUIT model has some core elements and assumptions [16, 15]. This FRUIT model's central

element is a spatial-temporal distribution of aircraft counts, since aircraft are not uniformly distributed in space or time. The approach taken to appropriately distribute these counts was to use flight plan data containing departure times, origins, and destinations of nearly every aircraft in the world grouped in UTC hourly files to reconstruct the spatial-temporal distribution of aircraft. The primary assumption here is that aircraft don't generally spontaneously appear into the airspace, but are rather coming from some known airport and travelling to another one.

Additionally, planes can be modeled as flying great circle routes (shortest distance over the earth). The expected airspeed of the aircraft can be estimated as a function of the distance between the two airports such that the greater the distance, the higher the expected average aircraft velocity. With virtual aircraft in the simulation departing at defined times to defined places using expected velocity and trajectories from a global fight plan database containing 3579 world-wide airports, the spatial-temporal aircraft counts can simply be "measured" over a global grid. The grid spacing used in this model is 1 degree by 1 degree over the WGS-84 earth model. Although these 1 degree dimensions have varying lengths by latitude, it's a relatively simple and effective grid to use.

The aircraft counts are such that any aircraft that passes near or through a grid point (rounding the decimal coordinates to the nearest value) are counted in one minute time window bins. The peak 1 minute "instantaneous aircraft count" then becomes associated with a given UTC hour at that grid point location. One minute time windows were chosen since although many aircraft may pass over a grid point within an hour, only those that are there within one minute of each other should be considered "clustered" in time and space where transmitted messages can be assumed to be coming from a group. The UTC hour count is set to the worst-case minute so that within a region, for every tile, there is an assigned worst minute for that tile (inherently a conservative estimate).

The result of this aggregated aircraft count can be seen in Figure 3 where tile index ($t_i$), given by:

$$t_i = 360 \cdot (90 + \Phi_i) + \Lambda_i$$

where $-90 \leq \Phi_i \leq 90$ is the latitude

$0 \leq \Lambda_i \leq 360$ is the eastward longitude of the $i^{th}$ tile

The tile index is along the left horizontal axis and the UTC hour of the day is on the right horizontal axis and the 1 minute peak aircraft counts in each hour is the vertical axis. The peak tile in Figure 3 ($t_i$ = 47446, $\Phi_i = 41°$, $\Lambda_i = 286°$), correlates with the same aircraft density hotspot observed in prior work (near JFK airport) where the density was measured with archived ADS-B aircraft data [21].

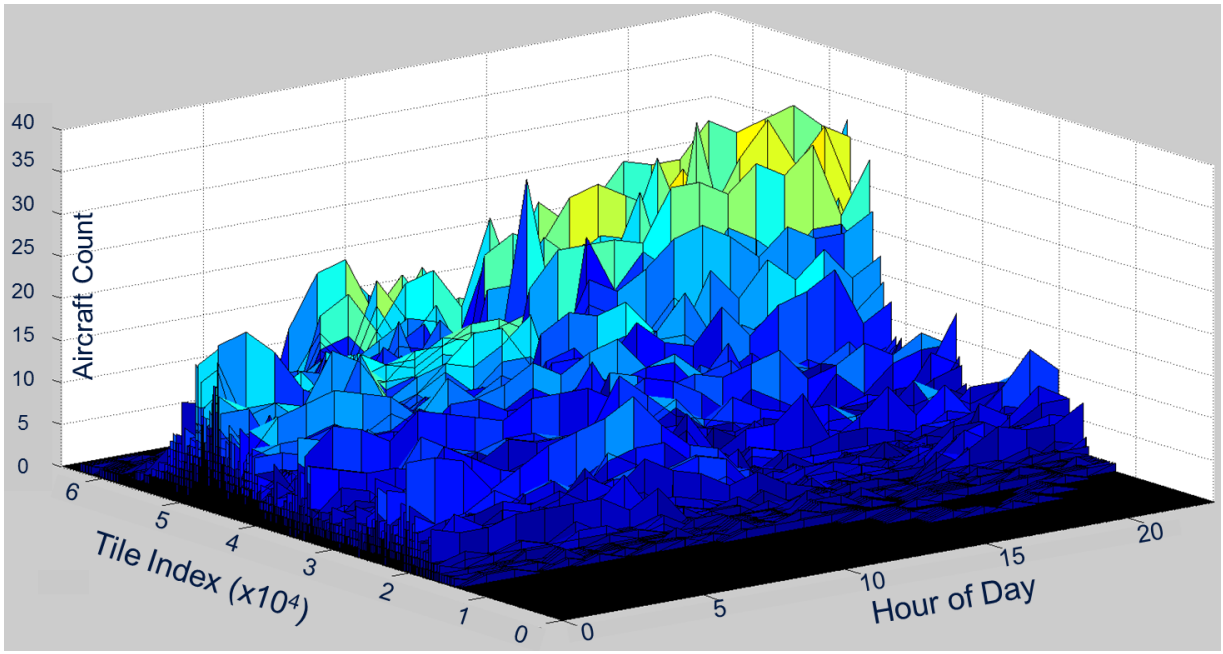


**Figure 3. ADS-B Message $P_d$ vs. Message Arrival Rate**

### *Avionics Transmit Message Rates*

Now that the aircraft counts are distributed in space and time in the model, the next step is to convert aircraft counts to categorized expected transmitted message rates. This step is typically performed during an applicable hour of analysis such that the spatial profile is two-dimensional and is assumed not to vary appreciably over time within the hour. This assumption accounts for the fact that the model applies the worst-cast traffic in each tile (e.g. a max-max case is held steady over the simulation hour). For example, if FRUIT impact analysis is being assessed at 12:23Z, then the 12th hour aircraft count profile, $\kappa(t_i, h)$, would be used.

The aircraft counts in this profile need to be categorized by link type and transmit power. Furthermore, the transmitted messages must also be distributed between a top and bottom antenna where applicable. Table 1 and Table 2 describe this FRUIT model's assumptions of aircraft transmissions that enables a mapping from aircraft counts to message rates in each respective category. These values were determined through a careful analysis of the aircraft population in the US Northeast in combination with assumptions about TCAS and SSR reply rates [17] given the average aircraft density and radar density in that region [22]. Furthermore, the assumptions in Table 1 are consistent with results from other studies [17, 15].

**Table 1. Aircraft Transmitter Categorization Assumptions**

| Parameter | Symbol | Value |
|---|---|---|
| Fraction ATCRBS | $\nu_{ATCRBS}$ | 0.1 |
| Fraction Mode S | $\nu_{Mode\ S}$ | 0.9 |
| Fraction of Mode S that has ADS-B | $\nu_{ADS-B}$ | 0.3 |
| ADS-B msgs/s/aircraft | $\omega_{ADS-B}$ | 6 |
| Mode S short msgs/s/aircraft | $\omega_{Mode\ S}$ | 6 |
| ATCRBS msgs/s/aircraft | $\omega_{ATCRBS}$ | 60 |
| ADS-B Fraction of Top transmit | $\alpha_{ADS-B}$ | 0.5 |
| Mode S Fraction of Top transmit | $\alpha_{Mode\ S}$ | 0.5 |
| ATCRBS Fraction of Top transmit | $\alpha_{ATCRBS}$ | 0 |

**Table 2. Aircraft Transmitter Power Assumptions**

| Link Tech | Symbol | 125W | 250W | 500W |
|---|---|---|---|---|
| ADS-B | $\eta_{ADS-B}$ | 0.25 | 0.5 | 0.25 |
| Mode S | $\eta_{Mode\ S}$ | 0.54 | 0.3 | 0.16 |
| ATCRBS | $\eta_{ATCRBS}$ | 1 | 0 | 0 |

Although these parameters will have their own spatial and temporal distribution, this FRUIT model uses these values for "worst case" purposes. Over the ocean, there will certainly be a lower percentage of ATCRBS and low power transmitters, but there will also be a lower aircraft count and redistributing the categorization would therefore have a negligible effect. These tables are assumed to be representative of the populations in high aircraft density regions where the FRUIT model would have more impact on SBA Pd. In order to find the transmitted message count in a particular category, one must simply multiply the respective coefficients together. For example, the following equations show how to assess the expected number of transmitted messages per second at the lowest level of categorization using the variables in Tables 1 and 2 with $\kappa$ being the count profile:

$$\varphi_{ADS-B,Top,125W}(t_i, h) = \kappa(t_i, h) \cdot \nu_{ModeS} \cdot \nu_{ADS-B} \cdot \omega_{ADS-B} \cdot \alpha_{ADS-B} \cdot \eta_{ADS-B,125W}$$

$$\varphi_{ADS-B,Bottom,125W}(t_i, h) = \kappa(t_i, h) \cdot \nu_{ModeS} \cdot \nu_{ADS-B} \cdot \omega_{ADS-B} \cdot (1 - \alpha_{ADS-B}) \cdot \eta_{ADS-B,125W}$$

## V. Aggregation of Parameters for Instantaneous $P_{env}$ Calculation

Once the aircraft counts profile has been translated to transmitted messages per second in each respective category, the SBA receiver model can apply a phased array beam gain pattern over an area and determine the environmental impact to $P_d$ [16]. Figure 4 shows an example of a notional SBA receiver beam "footprint" (extent of $E_b/N_0$ gain above required link margin) overlaid on the tile grid space. When evaluating the impact of FRUIT to the ADS-B aircraft of interest in this beam during a particular hour of the day, the methods described in Section 3 can be used to determine the categorized transmitted message rates for each grid point within the beam's footprint. To determine the effective message rates that would be "received" by the beam and have impact on the ADS-B messages of interest, equation (eq. 2) can be expanded to account for each λ value (when combined with the appropriate τ) in equation (eq. 1) as follows:

$$\varphi_{ModeS}(h) = \sum_{i=1}^{n}\left[\sum_{j=125W,250W,500W}\left(\varphi_{ModeS,Top,j}(t_i, h) \cdot \gamma_{Top,j} + \varphi_{ModeS,Bottom,j}(t_i, h) \cdot \gamma_{Bottom,j}\right)\right] \quad (2)$$

This is calculated similarly for $\varphi_{ATCRBS}$ and $\varphi_{ES}$ in order to populate $P_{env}$ which is the scaling factor of equation (eq. 1). The value of $P_{env}$ can be used to determine the effective $P_d$ of any given ADS-B message that was transmitted in that beam during a given time window where the ADS-B message's clear sky probability of successful reception is $P_R$.

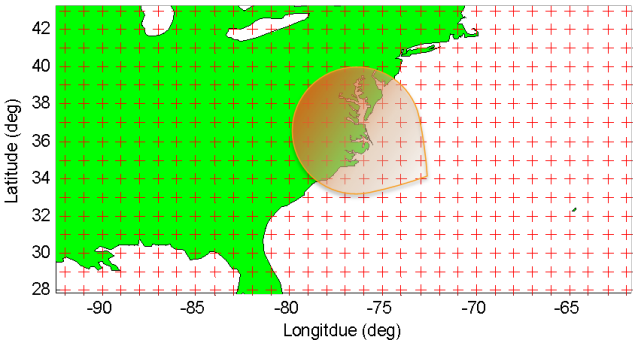


**Figure 4. Ex. of SBA Beam Footprint over Tiles**

# VI. Performance Evaluation

### *Performance Evaluation Criteria*

The performance/compatibility of a SBA system relative to active 1090 MHz in-band signals-in-space depends on the level of surveillance/tracking service that one is attempting to achieve. For example, an aircraft tracking service (as opposed to surveillance service) such as ADS-C (which is out-of-band of 1090 MHz and is a substantially different protocol and link technology compared to ADS-B [23]) only provides state vector reports on aircraft approximately every 14 minutes for suitably equipped oceanic flights. However, this 14 minute reporting interval is sufficient to support track-based longitudinal separation services greater than or equal to 30 NM in certain regions [24].

In Aireon's case, the service being advertised will be capable of supporting continuously global, near real-time surveillance for a 15s update interval (UI) greater than or equal to 95% of the time for oceanic and low-density aircraft environments. Notionally, with proper communications and navigation performance available, this 15s UI performance could support 10 NM or less separation services depending on the outcome of the ICAO and regional Air Navigation Service Provider (ANSP) safety case assessments. Currently, Eurocontrol's GEN-SUR document describes terrestrial En-Route (5 NM) and Terminal (2-3 NM) surveillance applications requiring 8s and 5s UIs, respectively [25]. However, there are also applications currently using longer UIs for 5 NM separation (the FAA uses 12s long range radars) and others being developed, such as Pairwise Trajectory Management, that may support En-Route separation, given proper equipage, with significantly less stringent ATC UI requirements than those in the GEN-SUR [26].

Therefore, for the sake of simplicity, the criterion for the evaluation of performance of Aireon's core mission is for the 15s UI to be met greater than or equal to 95% for 125W equipped aircraft with a top-mounted or diversity antenna (diversity antennas are required for TCAS operations and aircraft that operate above 18,000').

### *Performance Evaluation Tool and Results*

Since LEO satellite motion and beam positions rapidly change over time, ~3.6 NM/s, a stochastic simulator was created for Aireon by Exelis called ASIM. This simulator accounts for the dynamic aspects of the system for a higher fidelity assessment of the expected UI performance. ASIM was configured to apply the FRUIT model described in the earlier sections of this paper and to place "test" aircraft at specific fixed locations (each location gets a 125W and a 250W equipped aircraft) with a conservative antenna pattern. Using this configuration ASIM calculated the UI statistics over a 24 hour period for each tile and each transmit power type.

Although any and every point on the earth could be evaluated, the test aircraft were placed in oceanic/low-density airspace most proximate to the 20 busiest airports in the world (see Figure 5) according to Wikipedia (data provided by Airports Council International) [27]. It was expected that one or more of these tiles would be subject to beams with significantly high aircraft density and FRUIT impacts and would represent the worst case UIs for ADS-B surveillance services. Since Aireon's hosted payload will be mounted to the Iridium NEXT satellites that have less overlapping coverage near the equator, a test aircraft was also added near airports in Ecuador.

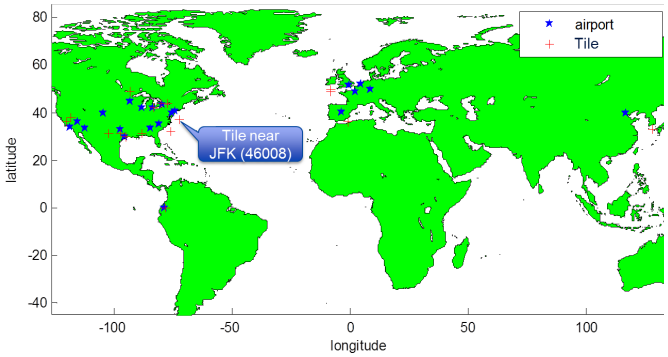


**Figure 5. Highest Density Airports and Neighboring Tiles**

ASIM evaluates the instantaneous probability of detection of each aircraft message as described in sections1-5 for each beam. For Aireon, there are many instances of beam overlap and satellite-to-satellite overlap, particularly north of the Tropic of Cancer and south of the Tropic of Capricorn, and this results in a higher aggregate $P_d$ for transmitted messages since these receptions are independent of each other and the gain/interference profiles are often different. The Update Interval (UI) is calculated relative to position message updates and ASIM accounts for the mix of odd and even parity position messages using the ADS-B 1090ES compact position reporting (CPR) algorithm [14]. The theoretical minimum aggregate average $P_d$ necessary to support a 15s UI at 95% can be computed as follows:

$$(1 - P_{UI}) = (1 - P_d)^{(T_{UI} * f_{position\_tx})}$$

where:

$P_{UI}$ = 0.95 (required $P_d$ of the position message within the UI timeframe)

$T_{UI}$ = 15s (required UI timeframe)

$f_{position\_tx}$ = 2 Hz (rate of position information transmitted from the aircraft)

Solving this equation for $P_d$ gives a value of 0.095, which is the minimum average $P_d$ of any given ADS-B message. Indeed, such $P_d$ has been exceeded with observations from a prototype SBA receiver with a single beam [28, 29]. The Aireon payload has the capability to support multiple simultaneous beams to support wide coverage areas. Figure 6 and Figure 7 show the UI results for the 17 test tiles for the 125W and 250W aircraft, respectively. Although the transmit power of the ADS-B aircraft makes a substantial difference in the results, all 15s UI percentages are above 95%, thus meeting the stated criterion for Aireon's core mission and demonstrating its advertised performance and compatibility with the 1090 MHz in-band environment (FRUIT) model.


**Figure 6. ADS-B UI results for 125W Equipped Aircraft in the Top 17 High Density Tiles**

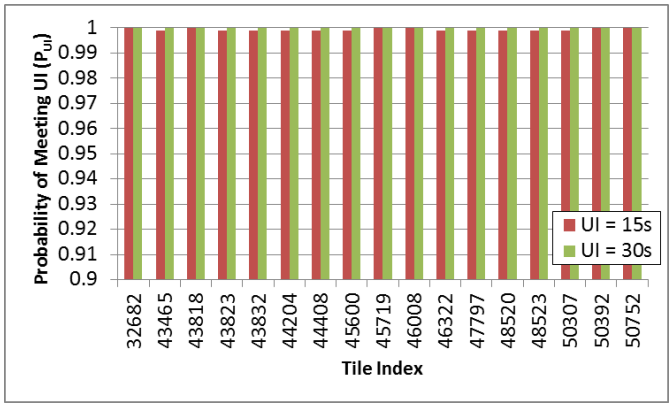


**Figure 7. ADS-B UI results for 250W Equipped Aircraft in the Top 17 High Density Tiles**

## VII. Conclusion

This paper presents a detailed account of Aireon stochastic 1090 MHz ADS-B co-channel interference model and simulation of its performance. Although the assumptions within the simulation will need to be calibrated upon the launch of the first two Aireon payloads in 2015, the majority of these assumptions are suitably conservative to allow for some unexpected errors. Clearly, if the model's assumptions are validated, the results shown in Figure 6 and Figure 7 demonstrate that 15 sec UI at 95% $P_d$ is achievable globally even in presence of FRUIT for 125W transmit power. A preliminary estimation of 8 sec UI performance in presence of FRUIT also show that a 95% $P_d$ is achievable in FIRs around the world even for 125W aircraft.

With respect to ongoing ITU efforts to protect 1090 MHz ADS-B from ground to space, a co-primary safety allocation for aircraft to Space-Based ADS-B (SBA) receivers would impose no additional in-band or out-of-band restrictions in support of global flight surveillance and tracking services since they are provisioned to co-exist with the 1090 MHz Aeronautical Radio Navigation Service (ARNS) environment. These results represent an in-depth and peer-reviewed analytical demonstration that Aireon will meet and/or exceed its planned UI performance in challenging regions. In addition, a novel and industry-inspired approach to characterizing and analyzing 1090ES co-channel interference has been shown. This methodology could also be leveraged to assess expected performance for other applications such as TCAS and ADS-B IN.

## References


[1] O. Gupta, "Global Augmentation of ADS-B Using Iridium NEXT Hosted Payloads," in ICNS Conference Proceedings, Herndon, VA, 2011.

[2] P. Noschese, S. Porfili and S. Di Girolamo, "ADS-B via Iridium NEXT Satellites," in ESAV Conference Proceedings, Rome, Italy, 2011.

[3] M. Carandente and C. Rinaldi, "Aireon Surveillance of the Globe via Satellite," in ESAV Conference, Rome, 2014.

[4] M. Castle, C. R. Sprouse and L. R. Bachman, "Analysis of 1090 MHz ES Ground Based Transceiver Performance in the LA 2020 Terminal Environment," Laurel, MD, 2005.

[5] E. M. Valovage, "A Method to Measure the 1090 MHz Interference Environment," in ICNS Conference Proceedings, Herndon, VA, 2009.

[6] NTIA, "Compendium for 960-1164 MHz," NTIA, 2014.

[7] RTCA, Inc., "Minimum Operational Performance Standards for ATCRBS Airborne Equipment," RTCA, 2008.

[8] NAVEDTRA, "Electronics Technician, Vol 4 - Radar Systems," US Navy, Pensacola, FL, 1993.

[9] Y. Guo, J. Yang and C. Guan, "A Mode 5 Signal Detection Method Based on Phase," in ICNC, Shenyang, 2013.

[10] R. Echevarria and L. Taylor, "Co-Site Interference Tests of JTIDS, EPLRS, SINCGARS, and MSE (MSRT)," in Tactical Communications Conference, Fort Wayne, IN, 1992.

[11] Northrup Grumman, "Understanding Voice and Data Link Networking," San Diego, CA, 2013.

[12] ICAO, "Annex 10, Vol IV, Surveillance and Collision Avoidance Systems," ICAO, 2014.

[13] RTCA, Inc., "MOPS for ATCRBS/Mode S Airborne Equipment," RTCA, 2008.

[14] RTCA, Inc, "Minimum Operational Performance Standards for 1090 MHz ES ADS-B and TIS-B," RTCA, 2009.

[15] Eurocontrol, "1090 MHz Capacity Study - Final Report," Eurocontrol, 2006.

[16] Exelis, Inc., "ASIM FRUIT Design Description Document," Exelis private communication, Herndon, VA, 2014.

[17] V. A. Orlando and W. H. Harman, "GPS-Squitter Capacity Analysis," no. ATC-214, 1994.

[18] A. Scarciglia, "1090 MHz Interference Problem," Exelis private communication, Herndon, VA, 2007.

[19] FAA, "ADS-B/ADS-R Critical Services Specification," US DOT, Washington, DC, 2014.

[20] J. Wollweber, "Impact of Frequency Assignment for ADS-B Reception via Satelliate on Terretrial ARNS," ICAO FMG, Brussels, Belgium, 2014.

[21] M. A. Garcia, J. Keller and J. Boughton, "ADS-B System Network Bandwidth and CPU Optimization," IEEE ICNS Conference Proceedings, 2013.

[22] J. Minnix and J. Stafford, "FRUIT Analysis Report," Exelis Private Communication, Herndon, VA, 2013.

[23] ICAO, Global Operational Data Link Document, Montreal, Canada, 2013.

[24] FAA, "NOPAC - Order JO 7110.65U," US DOT, 2014.

[25] Eurocontrol, "Safety & Performance Requirements Document on a Generic Surveillance

System Supporting ATC Services," Brussels, Belgium, 2015 (Pending).

[26] K. Jones, "Pair-Wise Trajectory Management-Oceanic CONOPS," NASA, 2014.

[27] Wikipedia, "World's Busiest Airports by Aircraft Movements," 1 2 2014. [Online]. Available: http://en.wikipedia.org/wiki/World's_busiest_airports_by_aircraft_movements. [Accessed 1 2 2014].

[28] H. Blomenhofer, A. Pawlitzki, P. Rosenthal and L. Escudero, "Space-Based Automatic Dependent Surveillance Broadcast (ADS-B) Payload for In-Orbit Demonstration," ASMS Conference Proceedings, vol. 6, pp. 160-165, 2012.

[29] K. Werner, J. Bredemeyer and D. T, "ADS-B over Satellite," Proceedings of ESAV, p. 55, 2014.

## Acknowledgements

The authors would like to thank Boris Veytsman, Antonio Scarciglia, and Stan Jones for their technical review and contributions to this paper. The authors would also like to thank NAV Canada, ENAV, IAA, NAVIAIR, and the FAA SBS Program Office for their support of the Aireon program.

## Email Addresses

Michael.Garcia@aireon.com

James.Stafford@exelisinc.com

Jay.Minnix@exelisinc.com

jdolan@regulus-group.com